AIAA JOURNAL
Vol. 45, No. 9, September 2007

Technical Notes

TECHNICAL NOTES are short manuscripts describing new developments or important results of a preliminary nature. These Notes should not exceed 2500 words (where a figure or table counts as 200 words). Following informal review by the Editors, they may be published within a few months of the date of receipt. Style requirements are the same as for regular contributions (see inside back cover).

Effect of Freestream Noise on Shock-Wave/Turbulent-Boundary-Layer Interactions

Julien Weiss* and Ndaona Chokani†
Duke University, Durham, North Carolina 27798

DOI: 10.2514/1.30083

Introduction

SHOCK-WAVE/turbulent-boundary-layer interactions (STBLI) with significant flow separation are known to be characterized by large-scale, low-frequency oscillations of the separation shock [1,2]. However, the physical mechanism driving the unsteady motion of the separation shock is still unknown. Several experimental results suggest that the large-scale, low-frequency shock motion is related to fluctuations in the incoming boundary layer upstream of the separation shock (e.g., [3]), whereas other results suggest that the shock motion is correlated to fluctuations in the recirculation region downstream of the shock (e.g., [4]).

Recent advances have enabled the computation of STBLI by means of direct numerical simulation (DNS) and large eddy simulation (LES). Rizzetta and Visbal [5] performed LES of Mach 3 compression ramp flows and compared their results with the experimental data of Dolling and Murphy [6]. The LES predicted high-frequency shock oscillations that were similar in magnitude to the characteristic frequency of the incoming boundary layer, but did not predict large-scale excursions of the shock that are observed in the experiments. The large-scale, low-frequency motion was not reproduced in the LES of Rizzetta and Visbal [5] or in the DNS of Adams [7]. On the other hand, the recent LES of Loginov et al. [8] shows the presence of large-scale motion of the separation shock; however, no estimate of the shock frequency is provided.

The mismatch between numerical and experimental results, together with the absence of a clear correlation between the large-scale, low-frequency shock motion and the upstream and downstream flow structure, has raised the speculation that the shock motion may be driven, at least in part, by some type of facility-dependent forcing [1]. In conventional high-speed wind tunnels, the freestream disturbances arise primarily from the aerodynamic noise that is generated in the turbulent nozzle wall boundary layer and then radiated in the form of fluctuating Mach waves into the freestream [9]. Only in the so-called quiet wind tunnels can the level of freestream disturbances be reduced by maintaining the nozzle boundary layer to be laminar [10].

The present work is the first experimental investigation of STBLI in a quiet wind tunnel. The objective is to determine whether the unsteady characteristics of the separation shock in a compression ramp flow is influenced by the level of freestream noise. Furthermore, the Reynolds number in the present study is sufficiently low that the measurements are suited for comparison to future DNS and/or LES.

Experimental Setup

The experiment is conducted in the Mach 3.5 Supersonic Low-Disturbance Tunnel (SLDT) at NASA Langley Research Center. The SLDT is a pressure-vacuum tunnel with a cross section of 152×254 mm at the nozzle exit plane. In the SLDT, the level of freestream noise can be varied by opening or closing the bleed valves that are located just upstream of the nozzle throat: operation with bleed valves open (BVO) results in a low level of freestream noise, whereas operation with bleed valves closed (BVC) results in a level of freestream noise that is comparable to conventional supersonic tunnels [10].

The STBLI is generated on a compression ramp model that is mounted horizontally along the tunnel centerline (Fig. 1). The flat plate has dimensions of 292×178 mm and the removable ramp is formed by a 24-deg wedge that is 38 mm in length. The wedge spans the width of the plate and no side fences are used. The exposed length of the ramp is 42 mm in length, or six times the incoming boundary-layer thickness.

Measurements are performed at a stagnation pressure of 1.38×10^5 Pa and a stagnation temperature of 300 K for both BVC (conventional) and BVO (quiet) conditions. To ensure that the laminar–turbulent transition on the flat plate occurs at the same location regardless of the freestream disturbance level, a 38-mm-wide transition strip made of no. 40 sandpaper is placed along the leading edge of the flat plate. Schlieren visualizations of the interaction show that the separation length L_s (distance between the ramp corner and the average position of the separation shock foot) is approximately 14 mm and unchanged for both BVO and BVC conditions.

Boundary Conditions

Freestream Disturbances

Measurements of the freestream disturbance levels in the empty test section are performed by traversing a hot-wire probe on the tunnel centerline; the compression ramp model is removed from the test section for these measurements. The hot wire is a Dantec 55P11 normal probe (diameter of 5 μm and length of 1 mm) that is operated with a Dantec Streamline constant-temperature anemometer equipped with a symmetrical bridge. The wire is operated at an overheat ratio of $a_w = 0.8$, and the frequency response of the system is flat up to about 100 kHz. Under these conditions, the anemometer is only sensitive to mass flux fluctuations [11]. The anemometer is calibrated in the freestream by varying the tunnel stagnation pressure at constant total temperature. Conversion of mass flux fluctuations to

Presented as Paper 3362 at the 36th AIAA Fluid Dynamics Conference and Exhibit, San Francisco, CA, 5–8 June 2006; received 28 January 2007; revision received 19 April 2007; accepted for publication 23 April 2007.

*Research Associate, Department of Mechanical Engineering and Materials Science; currently Bombardier Aerospace, P.O. Box 6087, Station Centre-Ville, Montréal, Québec N3C 3G9, Canada; julien.weiss@aero.bombardier.com. Member AIAA.

†Research Professor, Department of Mechanical Engineering and Materials Science; currently Institut für Energietechnik, Swiss Federal Institute of Technology, 8092 Zürich, Switzerland. Associate Fellow AIAA.

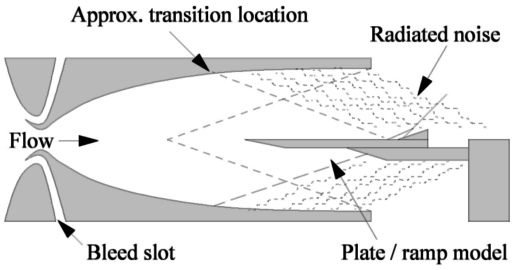

Fig. 1 Side view of experimental setup (schematic) with BVO.

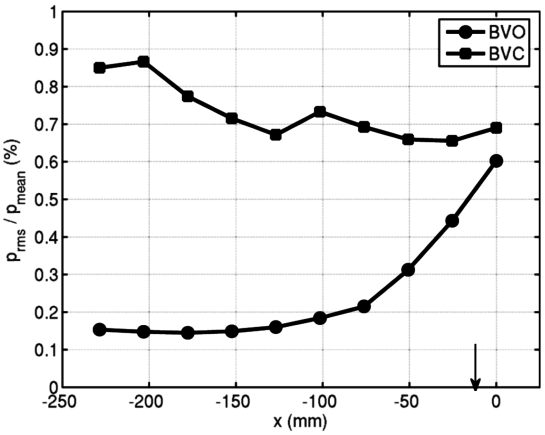

Fig. 2 Freestream disturbance level on the test section centerline ($y = 0$); bandwidth is 10 Hz–40 kHz; the arrow marks the average position of the separation shock foot; the origin $x = 0$ corresponds to the position of the ramp corner.

static pressure fluctuations is achieved following Laufer's method [9] with the assumption of stationary noise sources in the boundary layer.

The normalized static pressure fluctuation on the test section centerline ($y = 0$) is presented in Fig. 2 for BVO and BVC operation. The locations $x = 0$ and $x = -254$ mm correspond, respectively, to the locations of the ramp corner and the leading edge of the flat plate, when the compression ramp model is installed in the test section, and p_{rms} is obtained by integrating the power spectral density (PSD) of the static pressure fluctuations between 10 Hz and 40 kHz.

Under the present experimental conditions, the uncertainty in the fluctuating mass flux results is about $+10/-5\%$ [11]. For the BVC case, the assumption of stationary noise sources in the nozzle wall boundary layer likely results in a slight underestimation of the static pressure fluctuations; thus, we estimate the uncertainty in $p_{\text{rms}}/p_{\text{mean}}$ at $+15/-5\%$ [12]. For the BVO case, the disturbance levels presented in Fig. 2 are slightly higher than values reported in [10], because in the present anemometer system, the electronic noise cannot be subtracted from the signal; the low signal-to-noise ratio may result in an uncertainty of $+10/-50\%$ for the lowest values of $p_{\text{rms}}/p_{\text{mean}}$.

It is evident from Fig. 2 that in the BVO case, the freestream noise levels increase over the aft 100 mm of the model. Thus, with BVO, only the upstream half of the compression ramp model is situated in the SLDT's quiet core, which is free from acoustic radiation. On the other hand, the complete compression ramp model is immersed in acoustic radiation with BVC.

Figure 3 shows the PSD of the anemometer output voltage at $y = 0$ (test section centerline) and $x = 0$, -25, and -50 mm. These positions are close to the average position of the separation shock foot when the compression ramp model is installed in the test section. In Fig. 3, the area under each curve is equal to the variance of the signal. The signals are sampled at $f_s = 1$ MHz and the PSDs are calculated from 64 blocks of 8192 samples each. No windows are used in the calculation of the PSDs. With BVC, most of the energy is

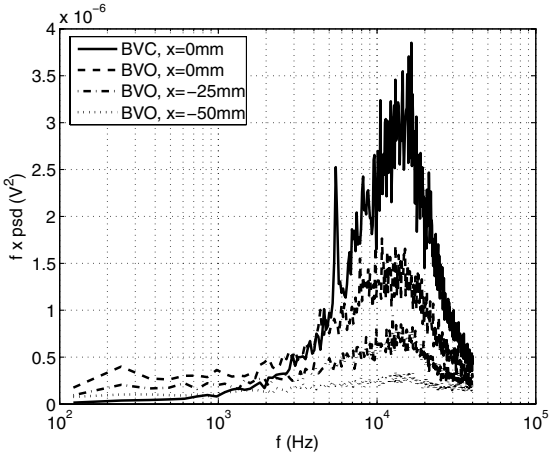

Fig. 3 Power spectral densities of freestream disturbances on the test section centerline ($y = 0$) at $x = 0$, -25, and -50 mm; the coordinate x is defined as in Fig. 2.

in a frequency band of 8–20 kHz; the PSD at $x = 0$ (ramp corner) is similar to the PSDs obtained at more upstream positions. With BVO, the energy present in the 8–20-kHz range progressively increases as the hot wire is traversed downstream. However, at $x = 0$, the energy in the 8–20-kHz range is only about half of that in the BVC case. Therefore, when the model is installed in the test section, although the total disturbance level at the ramp corner is almost as large for BVO as for BVC (Fig. 2), the acoustic energy in the dominant frequency band in the BVO case is only half of that in the BVC case.

Incoming Boundary Layer

Properties of the incoming boundary layer are measured on the plate centerline at $x = -13.5$ mm (the ramp is removed from the plate for these measurements). The mean flow properties are measured with a pitot probe, and the mass flux fluctuations are measured with the hot-wire anemometer described earlier.

The mean flow properties of the incoming boundary layer are summarized in Table 1. The Van-Driest-transformed velocity profiles are identical for BVO and BVC and show a small logarithmic region that is characteristic of a zero-pressure-gradient turbulent boundary layer. The profiles of mass flux fluctuations and the shape of the mass flux spectra are also identical for BVO and BVC. Thus, the properties of the incoming boundary layer are independent of the freestream noise levels.

Separation Shock Unsteadiness

The unsteady characteristics of the separation shock are measured with a cylindrical hot-film probe that is positioned above the incoming boundary layer ($y = 1.5\delta$) and then traversed, parallel to the plate, across the shock. The hot film is a Dantec 55R01 composed of a cylindrical quartz fiber (diameter of 70 μm and length of 3 mm) covered with a 0.1-μm-thick nickel film. The hot film is used because hot wires repeatedly broke in the harsh environment of the fluctuating shock. The probe is operated at an overheat of $a_w = 0.8$ with the previously described anemometer system and, in a manner similar to that used with the hot wire, is calibrated in the tunnel freestream. The frequency response, determined with an electrical square-wave test, is approximately 20 kHz.

Table 1 Mean flow properties of the incoming flat-plate boundary layer with BVO and BVC

U_∞, m/s	654
δ, mm	6.90
δ_1, mm	2.65
θ, mm	0.369
$c_f(-)$	2.05×10^{-3}
$Re_\theta(-)$	3.01×10^3

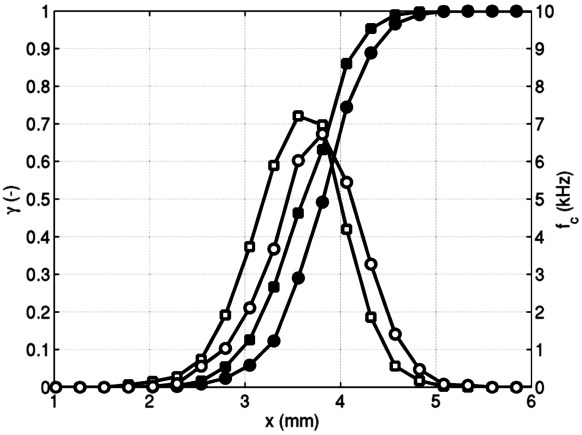

Fig. 4 Intermittency (solid symbols) and zero-crossing frequency (open symbols) of separation shock with BVO (circles) and BVC (squares); the x origin is arbitrary.

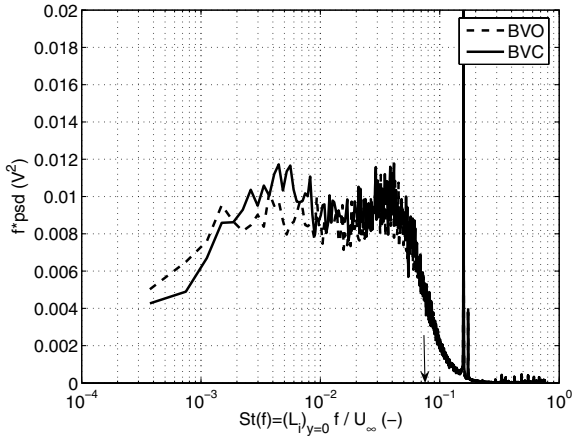

Fig. 5 PSD of the hot-film signal close to $\gamma = 0.5$; the arrow marks the cutoff frequency of the anemometer (20 kHz).

Examination of the hot-film time traces reveal that the signal is intermittent, due to the shock oscillation over the sensor: the mass flux is comparatively high (respectively low) when the sensor is positioned downstream (respectively upstream) of the shock. Quantitative information about the shock oscillation is obtained by converting the hot-film time traces into boxcar functions: for each sensor position, a threshold is set at the average value of the upstream and downstream mass flux and the shock is declared upstream (respectively, downstream) of the hot-film sensor whenever the instantaneous mass flux is larger (respectively, lower) than the threshold. Two statistical quantities are then obtained from the boxcar functions: the intermittency function $\gamma(x)$, which is the fraction of the time that the shock resides upstream of the measurement position, and the zero-crossing frequency $f_c(x)$, which is the number of times per second that the shock crosses, in one direction, the measurement position. It should be noted that the present method differs from the two-threshold method that is used when the separation shock motion is measured with wall pressure transducers [13]. The pressure transducers provide information about the motion of the shock foot, whereas the hot-film measures the oscillation of the separation shock in the freestream, above the incoming boundary layer. The main advantages of the present method over the more traditional wall pressure measurements is a better spatial resolution and a lower sensitivity to the threshold setting.

The intermittency and zero-crossing frequency of the separation shock are presented in Fig. 4 for BVO and BVC cases. The uncertainty in the probe x position is about 0.03 mm. In both cases, the maximum zero-crossing frequency occurs at $\gamma = 0.5$ and is close to $(f_c)_{\max} = 7$ kHz. Both the intermittency and the zero-crossing frequency curves are displaced approximately 0.2 mm downstream in the BVO case. This is most likely due to the fact that the tunnel stagnation pressure decreased by 2.5% when the bleed valves were opened; a decrease in stagnation pressure may reduce the average separation length L_s and thus the average position of the separation shock. The intermittent length, defined as the distance between the positions in which $\gamma = 0.05$ and $\gamma = 0.95$, is $L_i = 1.5$ mm for both BVO and BVC cases.

Dupont et al. [14] measured the characteristics of the separation shock motion in an incident shock interaction at $Ma = 2.3$ and $Re_\theta \sim 6900$ using both wall pressure transducers ($y/\delta = 0$) and a hot wire traversed above the incoming turbulent boundary layer ($y/\delta = 1.36$). Their results show that the frequency of the shock motion is independent of the distance from the wall. The intermittent length, however, decreases with increasing distance from the wall: at $y/\delta = 1.36$, the intermittent length is roughly 60% smaller than at $y/\delta = 0$. Assuming that the reduction of L_i is independent of the Mach number and the flow geometry, the intermittent length of the separation shock foot in the present experiment is approximately $(L_i)_{y=0} \sim 1.5/0.6 = 2.5$ mm or $(L_i)_{y=0}/L_s = 0.17$. The latter value is within the range of results compiled by Dussauge et al. [2] for different STBLIs.

Gonsalez and Dolling [15] showed that the Strouhal number based on the intermittent length of the separation shock foot, the maximum zero-crossing frequency, and the freestream velocity has a constant value of $St = (L_i)_{y=0}(f_c)_{\max}/U_\infty = 0.022$ in a broad range of separated STBLIs at Mach 5 and $Re_\theta = 31,600$. The present values of $(L_i)_{y=0} = 2.5$ mm, $(f_c)_{\max} = 7$ kHz, and $U_\infty = 654$ m/s yield $St = 0.027$ for both BVO and BVC cases.

The PSDs of the hot-film signal at the position closest to $\gamma = 0.5$ are presented in Fig. 5 for BVO and BVC. The arrow marks the hot-film cutoff frequency. The shape of the spectra should be only interpreted qualitatively, because the frequency response of hot-film anemometers is generally not flat up to the cutoff frequency. Nevertheless, both spectra overlap over the whole bandwidth, indicating that there is no effect of freestream noise on the separation shock dynamics. Given that the intermittent length and the zero-crossing frequency of the shock are also independent of the freestream disturbances, we conclude that the unsteady characteristics of the separation shock are not affected by the freestream noise level.

Conclusions

The effect of freestream noise on the unsteady characteristics of the separation shock motion in a separated compression ramp flow is investigated in the Supersonic Low-Disturbance Tunnel at NASA Langley Research Center. With BVC, the level of freestream disturbances is comparable to that usually obtained in conventional wind tunnels. With BVO, the acoustic energy of freestream disturbances in the region of separation shock unsteadiness is half of that obtained with BVC in the dominant frequency band.

Results show that the unsteady characteristics of the separation shock motion are independent of the level of freestream disturbances. The shock is characterized by large-scale, low-frequency oscillations that are comparable to those observed in previous experiments performed in conventional facilities at higher Reynolds number [1]. The intermittent length of the separation shock foot at the wall is obtained by rescaling measurements taken over the incoming boundary layer using the incident shock results of Dupont et al. [14]. Assuming that this scaling holds for the present flow, the Strouhal number based on the intermittent length of the separation shock foot, the maximum zero-crossing frequency, and the freestream velocity has a value of $St = 0.027$ for both BVO and BVC conditions. This value is very close to that obtained by Gonsalez and Dolling [15] for a broad range of STBLIs in a conventional tunnel. Therefore, wind-tunnel freestream noise does not appear to be the source of the discrepancies between experiment and simulation that have been previously reported.

Acknowledgments

This work was supported in part by the U.S. Air Force Office of Scientific Research under grants FA95550-04-1-0397 and FA9550-05-1-0178, monitored by John D. Schmisseur. The support of Fang-Jenq Chen, Rudolph A. King, Catherine B. McGinley, Hugh T. Pinkston, and Stephen P. Wilkinson of NASA Langley Research Center during the conduct of the experiments is very much appreciated. The efforts of Meelan M. Choudhari, Susan A. Gorton, and William L. Sellers III at NASA Langley Research Center to provide access to the facilities in the Flow Physics and Control Branch are gratefully acknowledged.

References

[1] Dolling, D. S., "Fifty Years of Shock-Wave/Boundary-layer Interaction Research: What Next?," *AIAA Journal*, Vol. 39, No. 8, 2001, pp. 1517–1531.

[2] Dussauge, J. P., Dupont, P., and Debiève, J.-F., "Unsteadiness in Shock Wave Boundary Layer Interactions with Separation," *Aerospace Science and Technology*, Vol. 10, No. 2, 2006, pp. 85–91.

[3] Beresh, S. J., Clemens, N. T., and Dolling, D. S., "Relationship Between Upstream Turbulent Boundary-Layer Velocity Fluctuations and Separation Shock Unsteadiness," *AIAA Journal*, Vol. 40, No. 12, 2002, pp. 2412–2422.

[4] Thomas, F. O., Putnam, C. M., and Chu, H. C., "On the Mechanism of Unsteady Shock Oscillation in Shock Wave/Turbulent Boundary Layer Interactions", *Experiments in Fluids*, Vol. 18, No. 1, 1994, pp. 69–81.

[5] Rizzetta, D. P., and Visbal, M. R., "Large-Eddy Simulation of Supersonic Compression-Ramp Flows," AIAA Paper 2001-2858, June 2001.

[6] Dolling, D. S., and Murphy, M. T., "Unsteadiness of the Separation Shock Wave Structure in a Supersonic Compression Ramp Flowfield," *AIAA Journal*, Vol. 21, No. 12, 1983, pp. 1628–1634.

[7] Adams, N. A., "Direct Simulation of the Turbulent Boundary Layer Along a Compression Ramp at $M = 3$ and $Re_\theta = 1685$," *Journal of Fluid Mechanics*, Vol. 420, Oct. 2000, pp. 47–83.

[8] Loginov, M. S., Adams, N. A., and Zheltovodov, A. A., "Large-Eddy Simulation of Shock-Wave/Turbulent Boundary Layer Interaction," *Journal of Fluid Mechanics*, Vol. 565, Oct. 2006, pp. 135–169.

[9] Laufer, J., "Aerodynamic Noise in Supersonic Wind Tunnels," *Journal of the Aeronautical Sciences*, Vol. 28, No. 9, 1961, pp. 685–692.

[10] Chen, F.-J., Malik, M. R., and Beckwith, I. E., "Comparison of Boundary Layer Transition on a Cone and Flat Plate at Mach 3.5," AIAA Paper 88-0411, Jan. 1988.

[11] Smits, A. J., "An Introduction to Constant-Temperature Hot-Wire Anemometry in Supersonic Flows," *The Heuristics of Thermal Anemometry*, FED Series, Vol. 97, American Society of Mechanical Engineers, New York, June 1990, pp. 35–40.

[12] Weiss, J., Knauss, H., and Wagner, S., "Experimental Determination of the Free-Stream Disturbance Field in a Short-Duration Supersonic Wind Tunnel," *Experiments in Fluids*, Vol. 35, No. 4, 2003, pp. 291–302.

[13] Dolling, D. S., and Brusniak, L., "Separation Shock Motion in Fin, Cylinder, and Compression Ramp-Induced Turbulent Interactions," *AIAA Journal*, Vol. 27, No. 6, 1989, pp. 734–742.

[14] Dupont, P., Haddad, C., and Debiève, J.-F., "Space and Time Organization in a Shock-Induced Separated Boundary Layer," *Journal of Fluid Mechanics*, Vol. 559, July 2006, pp. 255–277.

[15] Gonsalez, J. C., and Dolling, D. S., "Correlation of Interaction Sweepback Effects on the Dynamics of Shock-Induced Turbulent Separation," AIAA Paper 93-0776, 1993.

N. Clemens
Associate Editor